

ADVANCED MATERIALS

Supporting Information

for *Adv. Mater.*, DOI: 10.1002/adma.201606662

A Solution Processable High-Performance Thermoelectric
Copper Selenide Thin Film

*Zhaoyang Lin, Courtney Hollar, Joon Sang Kang, Anxiang
Yin, Yiliu Wang, Hui-Ying Shiu, Yu Huang, Yongjie Hu,*
Yanliang Zhang,* and Xiangfeng Duan**

Supporting Information for

A Solution Processable High-Performance Thermoelectric Copper Selenide Thin Film

Zhaoyang Lin, Courtney Hollar, Joon Sang Kang, Anxiang Yin, Yiliu Wang, Hui-Ying Shiu, Yu Huang, Yongjie Hu,* Yanliang Zhang,* and Xiangfeng Duan*

Dr. Z. Lin, Dr. A. Yin, Y. Wang, Prof. X. Duan
Department of Chemistry and Biochemistry
California NanoSystems Institute
University of California, Los Angeles, California 90095, United States
E-mail: xduan@chem.ucla.edu

C. Hollar, Prof. Y. Zhang
Department of Mechanical and Biomedical Engineering
Boise State University, Idaho, 83725, United States
E-mail: yanliangzhang@boisestate.edu

J. S. Kang, Prof. Y. Hu
Department of Mechanical and Aerospace Engineering
University of California, Los Angeles, California 90095, United States
E-mail: yhu@seas.ucla.edu

H. Shiu, Prof. Y. Huang
Department of Materials Science and Engineering
California NanoSystems Institute
University of California, Los Angeles, California 90095, United States

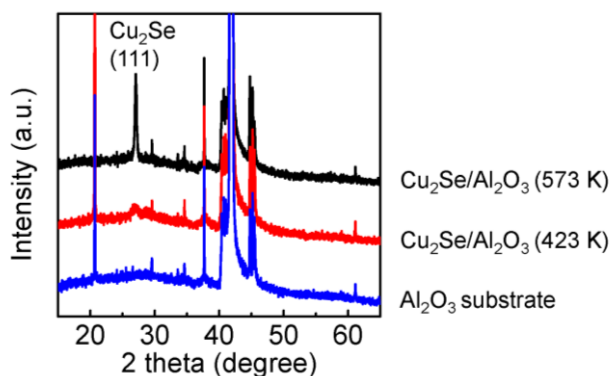


Figure S1. XRD pattern of the pure Al₂O₃ substrate, Cu₂Se/Al₂O₃ annealed at 423 K and 573 K.

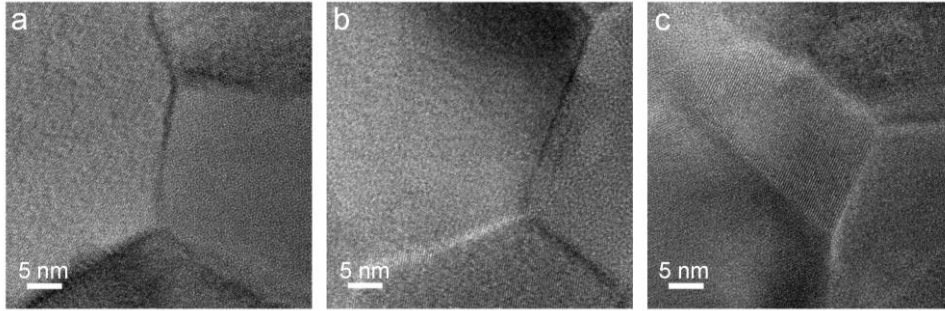


Figure S2. TEM images showing the polycrystalline nature and grain boundary of the fabricated film.

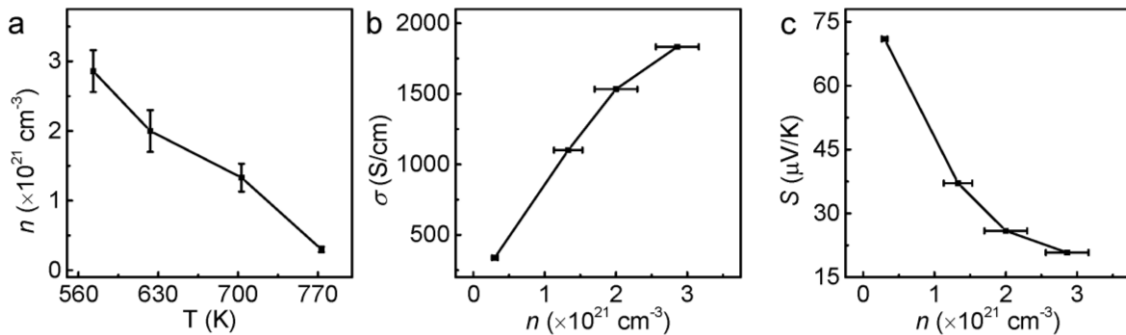


Figure S3. The effect of thermal annealing on the thermoelectric performance. (a) The room-temperature carrier concentration in the Cu_2Se thin film annealed at various temperature. (b) The dependence of electrical conductivity on the carrier concentration in the film. (c) The dependence of Seebeck coefficient on the carrier concentration in the film.

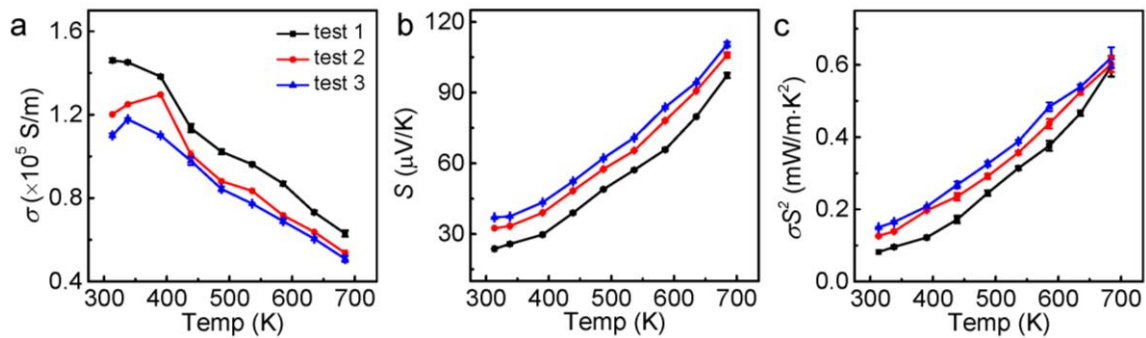


Figure S4. The cycling test of thin film Cu_2Se thermoelectric performance. (a) electrical conductivity σ , (b) Seebeck coefficient S , and (c) power factor σS^2 .

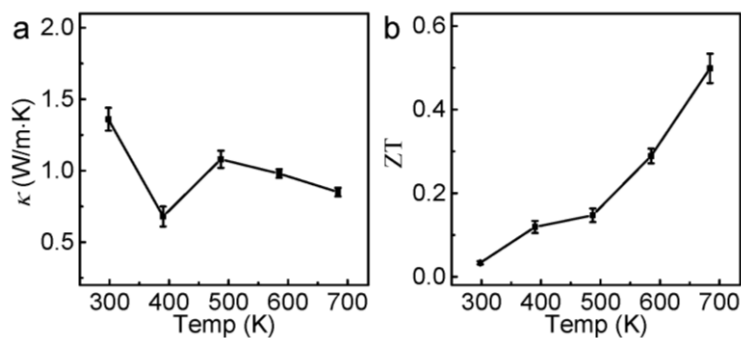


Figure S5. The temperature-dependent thermal conductivity κ (a) and the calculated ZT (b) for the Cu₂Se thin film.

Note. S1. Technical details for TDTR technique: The basic set-up is presented in our previous report (*Nat. Nanotechnol.* **2015**, 10, 701-706). A tunable Ti:sapphire laser emits a train of ~100 fs pulses at a repetition rate of 80.7 MHz and a central wavelength of 800 nm. The beam is divided into pump and probe beams by the polarized beam splitter (PBS), with a large power ratio between the two beams. The pump beam (with spot size of 50 μm) passes through an electro-optic modulator (EOM) with a sine-wave modulation up to 20 MHz and then through a bismuth triborate (BIBO) crystal, where its frequency is doubled to 400 nm, resulting in the pump beam heat up the sample surface with sine-wave oscillation. The probe beam (with spot size of 10 μm) is controlled with a delay time (up to 6 ns) by a mechanical delay stage, and it is excited to sample surface with coaxial geometry with pump beam. The reflected intensity from probe beam is measured by a photodiode detector (Thorlabs PDA36A). Both photodiode and EOM are connected with lock-in amplifier and it allows to detect signal only from the reference frequency. The surface temperature of sample ($\Delta T(t)$) is proportional with reflectance signal ($\varphi(t)$) of the surface ($\varphi \sim \Delta T$). We fit the experimental data with thermal model for thermal conductivity extraction from the model. Below is the mathematic description of the thermal model.

The temperature response from our lock-in amplifier is expressed by

$$Z(w_0) = \frac{\beta Q_{pump} Q_{probe}}{T^2} \sum_{k=-\infty}^{\infty} H(w_0 + kw_s) \exp(ikw_s \tau) \quad [1]$$

where β , Q_{pump} , Q_{probe} , T are the thermoreflectance coefficient, pulse power for pump beam, pulse power for probe beam, and period of pulse (both pump and probe), respectively. w_0 , w_s , τ , and k is the reference frequency, $2\pi/T$, time delay between pump and probe pulse, and transform variable, respectively. The impulse response H is expressed by following steps.

WILEY-VCH

In frequency domain, the heat flux and temperature of bottom side of material, θ_b and f_b , are expressed by

$$\begin{bmatrix} \theta_b \\ f_b \end{bmatrix} = \begin{bmatrix} \cosh(qd) & \frac{-1}{\sigma_z q} \sinh(qd) \\ \sigma_z q \sinh(qd) & \cosh(qd) \end{bmatrix} \begin{bmatrix} \theta_t \\ f_t \end{bmatrix} \quad [2]$$

Where θ_b , f_b , σ_z , and d are the heat flux of top side, temperature of top side, cross-plane thermal conductivity, and thickness of material. q is expressed by

$$q^2 = \frac{\sigma_r k^2 + \rho c i \omega}{\sigma_z} \quad [3]$$

where σ_r , ρ , c are the in-plane thermal conductivity, density of material, and heat capacity.

If multiple layered material,

$$\begin{bmatrix} \theta_b \\ f_b \end{bmatrix} = N_n N_{n-1} \cdots N_1 = \begin{bmatrix} A & B \\ C & D \end{bmatrix} \begin{bmatrix} \theta_t \\ f_t \end{bmatrix} \quad [4]$$

If bottom substrate is semi-infinite, $C\theta_t + Df_t = 0$. So, the top side temperature is expressed by

$$\theta_t = \frac{-D}{C} f_t \quad [5]$$

If we consider heat flux from pump beam on the top side and taking inverse Hankel transform,

$$\theta_t(r) = \int_0^\infty k J_0(kr) \left(\frac{-D}{C}\right) \frac{A_0}{2\pi} \exp\left(\frac{-k^2 w_0^2}{8}\right) dk \quad [6]$$

where A_0 and w_0 are the power of pump beam and pump beam diameter, respectively.

Consider probe beam intensity and finally $H(w)$ is expressed to

$$H(w) = \frac{A_0}{2\pi} \int_0^\infty \frac{-D}{C} \exp\left(\frac{-k^2 (w_0^2 + w_1^2)}{8}\right) dk \quad [7]$$

where w_1 are the probe beam diameter, respectively.